A STUDY OF CELLULOSE AND LIGNIN EXTRACTED FROM *SĀNCI* BARK AND THEIR MODIFICATION

ASADULLA ASRAF ALI, SHIRSA MAZUMDAR and ROBIN KUMAR DUTTA

Department of Chemical Sciences, Tezpur University, Tezpur 784028, Assam, India
✉ *Corresponding author: R. K. Dutta, robind@tezu.ernet.in*

Received January 11, 2023

Numerous studies have been carried out regarding different early and medieval writing bases like papyrus, birch bark, parchment, and Tālpātra. The quality of plant-derived manuscript writing bases has been aided by the presence of cellulose and lignin in plant cell walls. Sāncipāt, a popular writing base in early and medieval Assam, India, has not yet been thoroughly studied in this regard. In this paper, a scientific attempt has been made to reveal the physicochemical and mechanical properties of cellulose and lignin fibre in Sāncipāt. Various analytical techniques, including FTIR, P-XRD, TEM, UTM, were employed to characterize the cellulose fibres and lignin extracted from both old and new Sāncipāt, as well as their modified forms. A comparative analysis was made between the old and new bark samples of both cellulose fibres and lignin, and the general conclusions drawn from this work can be attributed to structural, thermal, and morphological changes of both cellulose fibres and lignin with degradation and decomposition, accompanied by ageing. The structural and chemical compositions of the extracted samples from the old and new barks were found to be almost identical, indicating only some minor degradation. While FTIR and UV spectroscopic analyses of the samples confirmed the successful extraction of cellulose fibres and lignin, electron microscopy and X-ray diffraction techniques allowed observing the structural and morphological changes that had occurred in the old bark samples as a result of ageing. Thermal stability studies and tensile strength measurements were also carried out to investigate the mechanical properties of the old and new bark samples.

Keywords: cellulose, lignin, *Sāncipāt*, *Sānci* bark, *Aquilaria malaccensis*, conservation of manuscript, degradation

INTRODUCTION

Cellulose and lignin are the most abundant biopolymers found in all types of plants, essential for providing structural rigidity.[1-5] The percentage content of cellulose and lignin vary in different types of plants according to their origin and growth conditions.[6] Both cellulose and lignin have complex structural features, on which a lot of ground is still to be covered.[7,8] A linear syndiotactic homopolymer like cellulose contains thousands of linear β (1→4) linked glucopyranose units, and each glucopyranose unit contains three highly reactive hydroxyl groups, which reflect some important properties, such as hydrophilicity, chirality and biodegradability.[9] Due to higher polarity, greater number of hydrogen bonds and crystalline nature, cellulose has chemical resistance properties, which make it difficult to process in its original state.[7,9]

The second most common biopolymer after cellulose, lignin, has a very complex structure.[10] In accordance with the unique characteristics of lignin, hardwood lignin contains guaiacyl (G) and syringyl (S) units in varying ratios, whereas softwood lignin primarily consists of guaiacyl (G) units.[5,10,11] Sometimes, a small amount of *p*-hydroxyphenyl propane units associated with *p*-coumaryl alcohol are found in both soft- and hardwood lignins.[12,13] Though many researchers have extensively studied the structure of lignin, to date, no proper structural evidence has been reported to confirm the above.[5,14] The lignin structure is highly complex due to functional groups like methoxyl, phenolic, and aliphatic hydroxyl-containing various linkages.[5] The lignin molecule has several common linkages, including β-O-4 ether linkages. Following these are additional ether and C-C linkages, such as α-O-4, β-5, 5-5, 4-O-5, β-1, and β- βĭ.[5,15] However, the major part of the lignin molecule contains hydrophilic, as well as hydrophobic functional moieties, which turns it into a very suitable biomacromolecule for various applications.[16,17]

The primary roles of cellulose and lignin in plant cell walls are to give them strength, rigidity, and stiffness.[2,4,5] The plant's defense against microbial attack is provided by lignin, which also plays a crucial role in the movement of water, minerals, and nutrients within the plant.[5] Based on this criterion, both cellulose and lignin are the key components that can have significant impact on the conservational aspects of different old manuscripts made from papyrus, Birch bark, *Tālpātra*, *Sāncipāt etc*.[7,18,19]

Most scientists focusing on paper conservation have already studied the influence of different environmental factors on the stability of cellulose.[18] It has been reported that factors, such as temperature, relative humidity, pollutants, high energy radiation, biological activity, oxidation and crosslinking of lignocellulosic materials, may play a crucial role in the longevity and also deterioration of paper.[18] However, these kinds of intrinsic investigations are yet to be done in the case of *Sāncipāt* manuscripts, since the use of *Sāncipāt* (made of bark of Sānci tree, *Aquilaria malaccensis* Lamk. syn. *Aquilaria agallocha* Roxb.) was geographically limited to Assam, India, where tens of thousands of such manuscripts still exist with their strength, glaze and ink intact, representing invaluable treasures of Assam's rich history, literature and cultural heritage.[19,20]

The authors have already carried out scientific investigations on *Sāncipāt* and were successful in providing clues to finding a sustainable conservative technique for preserving it.[19] However, before one can proceed with the preservation of *Sāncipāt* manuscripts, it is of immense importance to conduct a thorough study on both cellulose and lignin extracted from *Sāncipāt*, and perform a comparative analysis between extracted samples from both old and new *Sāncipāt* to gain a deeper understanding. There has been some research on surface modifications by inducing nanoparticles to make cellulose and lignin more reactive for use in various applications.[21-27] A thorough study has also been done on the changes that occurred when surface modification of cellulose and lignin, extracted from the bark of both old and new *Sānci* bark, was carried out with zirconium oxychloride.

Though centuries-old *Sāncipāt* manuscripts are treasures of a rich cultural and literary heritage of Assam, the tradition of *Sāncipāt* was limited only to a small geographical area in a developing country, compared to those of other kinds of medieval manuscripts and provably because of that hardly any scientific research has been done on conservation of these manuscripts. Passive conservation methods are not enough for *Sāncipāt* manuscripts, as there are tens of thousands of such manuscripts in villages and Satras (Vaishnavite monasteries), where the arrangement of passive environment is impractical and also because there are practices of reading these manuscripts regularly or occasionally. This prompted the authors to work for developing a method of conservation of *Sāncipāt* manuscripts, so that the manuscripts can be protected from further damage. The main goal of the current study was to understand the structural and morphological characteristics of the cellulose and lignin extracted from both fresh and old *Sānci* bark. By carrying out chemical modification of cellulose fibers and lignin with zirconium oxychloride, their surface, thermal, physical and chemical properties could be improved for various applications.[28] As such, attempts were also made to examine the possibility of modifying NBC and NBL materials with zirconium oxychloride to enhance their physicochemical properties, such as improving their mechanical strength by reinforcing the polymer matrices, biocompatibility and thermal stability.[28-30] In addition to that, we also wanted to examine the effects of natural degradation on both cellulose fiber and lignin structure and conformation by comparing cellulose fiber and lignin extracted from old and fresh *Sānci* barks.

EXPERIMENTAL

Materials

Both old and new *Sānci* barks were obtained from *Sānci* trees. New barks were collected from a *Sānci* grower (Mr. Gogoi) from Kakodonga, Golaghat, Assam, while old barks dating about 100 years old were acquired from Rupam Kumar Sarma from Bam Beseria, Tezpur. The *Sānci* barks had an average width and length of 7.0–8.5 cm and 23.5–25 cm, respectively. The selection procedure was designed to keep the chosen *Sānci* bark uniform. The chemicals, *i.e*., sodium hydroxide (NaOH) extrapure AR 98% (SRL), hydrogen peroxide (H_2O_2) 30% (Emplura), hydrochloric acid (HCl) 35% (Emplura), sulphuric acid (H_2SO_4) 98% (Merck), polyvinyl alcohol (GS Chemical Testing Lab and Allied Industries), zirconium oxychloride octahydrate ($ZrOCl_2.8H_2O$) extrapure 99.5% (SRL), polyvinyl alcohol (PVA), degree of polymerization 1700-1800 (GS Chemical Testing Lab and Allied Industries), and ethanol absolute 99.9% were used as received, without

additional filtration. The experiments were conducted using distilled water.

Methods

Both old and new *Sānci* barks, after removing the outer scales, were initially washed with tap water and soaked in distilled water overnight. They were then taken out and brushed to remove debris and dirt. After washing again in fresh water several times thoroughly, they were oven dried at 40 °C for 1 hour. The bark was then cut into small pieces of 0.5-1 cm in width and 4-5 cm in length. These small pieces of *Sānci* bark were used for extraction of cellulose and lignin.

Cellulose fiber extraction

The extraction method was adapted and modified from that developed by Fitriana *et al*., in accordance with TAPPI method T-429 and ASTM D-588 (Fig. 1).[31] Two extraction stages of alkaline and peroxide treatments were conducted to extract cellulose from raw *Sānci* bark. First, the freshly prepared 5 g *Sānci* bark was pre-treated with 500 mL of 2% w/v NaOH solution at 100 °C for 5 hours until the structure of the bark became mushy and compromised. The fibers obtained were light yellow in colour, and were washed several times to bring them to a neutral pH. The second stage involves bleaching the fibers to remove lignin and other impurities with 200 mL of 3% v/v H_2O_2 solution (prepared from 30% H_2O_2) at adjusted pH 9-10 with 0.5 M NaOH, temperature of 60 °C, and reaction time of 60 minutes. The fibers were resuspended in 200 mL of 3% v/v H_2O_2 solution under the same conditions until the fibers turned white in colour. The cellulose fibers were weighed after being washed with distilled water and oven dried at 50 °C. The cellulose fibers were kept in a desiccator at room temperature in a Petri dish.

For the sake of analysis, old bark cellulose was denoted as OBC, new bark cellulose – as NBC, old bark lignin – as OBL, new bark lignin – as NBL, and modified cellulose and lignin – as MC and ML, respectively.

Lignin extraction

Lignin was extracted as per the methodology described in TAPPI standard T222 (Fig. 1).[32] Accordingly, small pieces of the raw *Sānci* bark (1 g) were first taken in a beaker and 35% HCl (50 mL) was added in small increments, while stirring with a glass rod. The beaker was kept in an ice-cold water bath while adding the acid. Following that, 5 mL of 98% H_2SO_4 was added, and the mixture was stirred several times over a period of a few hours and allowed to stand overnight at room temperature. Following the fibers' dispersion, the mixture was diluted with 200 mL of distilled water before being boiled for 4 hours at 80 °C, while being frequently topped off with hot water. The insoluble substance (lignin) was then given an overnight standing period in the solution to settle. The solution was then decanted, centrifuged with a Remi R-8C, and washed with distilled water without disturbing the precipitate. The collected lignin was weighed, oven-dried at 50 °C, and kept in a desiccator in a Petri dish.

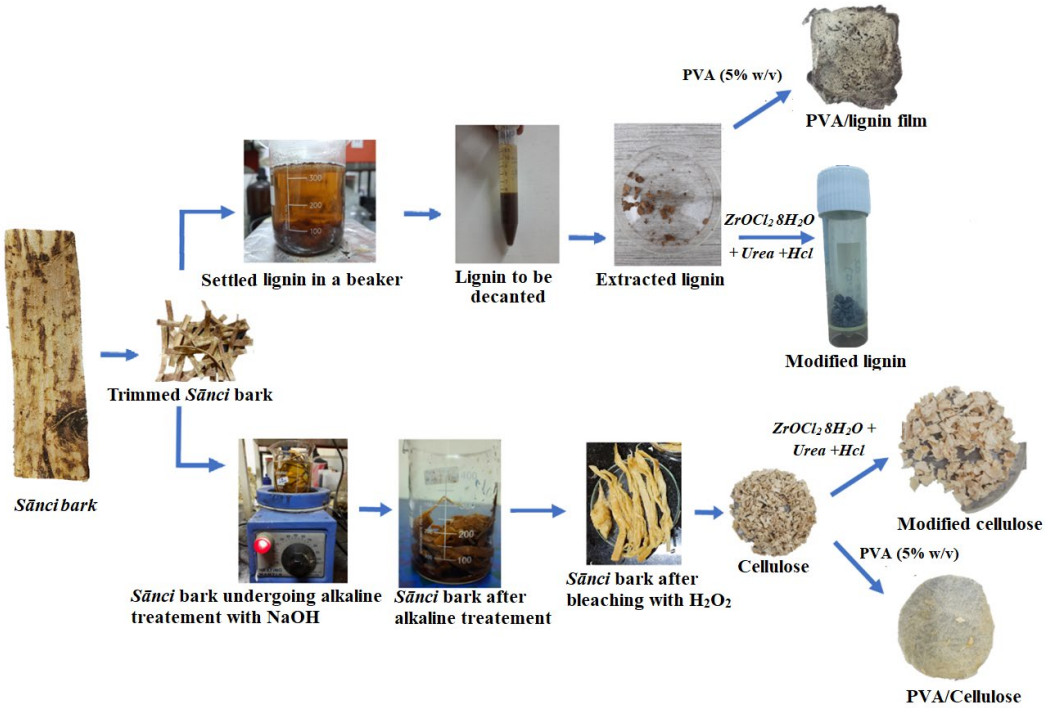

Scheme 1: A schematic presentation of the procedure in this work

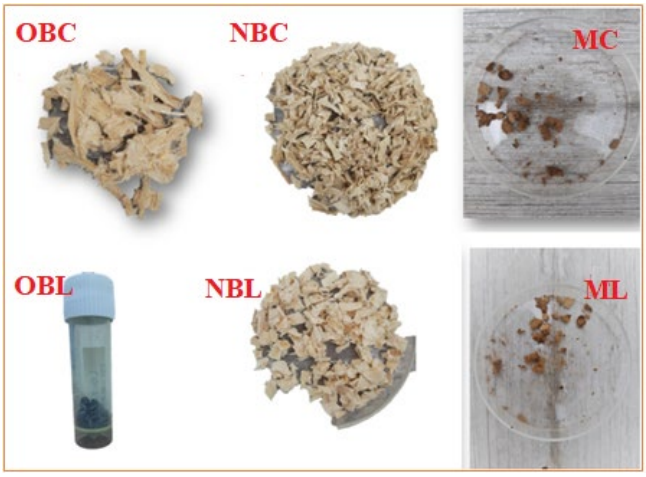

Figure 1: Cellulose from old bark (OBC), new bark (NBC); Lignin from old bark (OBL), new bark (NBL); modified cellulose (MC) and modified lignin (ML)

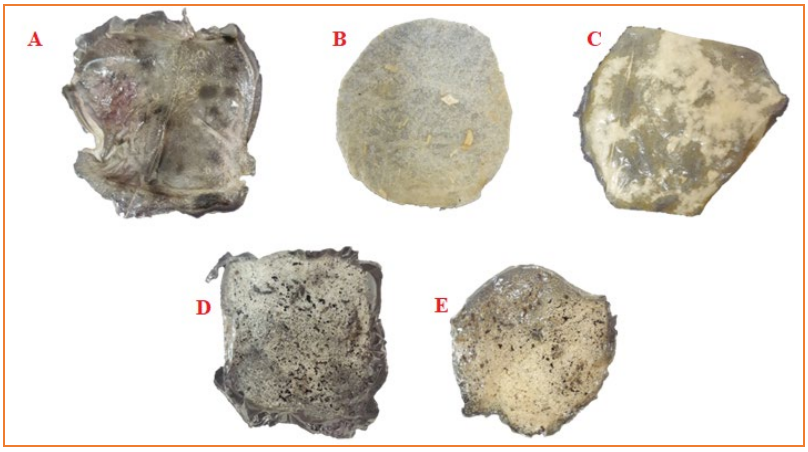

Figure 2: PVA (A), PVA/new cellulose film (B), PVA/old cellulose film (C), PVA/new lignin film (D) and PVA/old lignin film (E)

Preparation of modified cellulose fiber

New cellulose (NBC) fibers obtained from new *Sānci* bark were chemically modified according to the methodology of Mulinari *et al*. (Fig. 1).[21] This was accomplished by dissolving 2 g of zirconium oxychloride and 5 g of cellulose fibers obtained from *Sānci* bark in 100 mL of an aqueous hydrochloric acid solution (0.5 mol L^{-1}). Before being thoroughly washed with distilled water to remove all chloride ions (a negative silver nitrate test was performed to confirm the above) and filtered, the material was heated and precipitated with 10 g of urea, and then oven-dried for 24 hours at 50 °C. *Sānci* Cell/ZrO2.nH2O, also denoted as MC in shorthand, was the substance that was produced.

Preparation of modified lignin

New lignin (NBL) obtained from *Sānci* bark was chemically modified using the same method as that of cellulose modification (Fig. 1). The resulting substance was abbreviated ML, or *Sānci* Lig/ZrO2.nH2O. We are yet to elucidate an appropriate mechanism as to how nanoparticles are formed on the lignin surface.

Preparation of films

According to the procedure followed by Lim *et al*. in 1994, Frone *et al*. in 2011, and Posoknistakul *et al*. in 2020, PVA films, PVA/Cellulose fibers composite films and PVA/Lignin composite films were produced by casting aqueous solutions with 5% w/v PVA in distilled water respectively (Fig. 2).[30,31,33] PVA powder was gradually added to preheated distilled water, while being vigorously stirred at a rotational speed of 600 rpm for one hour, then heated at 80 °C for nearly three hours to completely dissolve the PVA. Using a Rivotek Ultrasonic cleaner, the final mixture was degassed for 15 minutes. The prepared PVA solution (50 mL) and the necessary amount of cellulose fibers (0.5 g) and lignin particles (0.5 g) were mixed in separate beakers to synthesize PVA/Cellulose fibers and PVA/Lignin composite films, respectively. The homogenous mixtures of PVA/cellulose fibers and PVA/lignin, along with the PVA solution alone, were placed in standard Petri dishes (150 mm x 15 mm) separately for three days at room temperature of 25 °C and relative humidity of 60% RH until the solvent completely

evaporated. PVA films of 1.00 mm thickness, PVA/Cellulose fibers composite films of 0.80 mm thickness and PVA/Lignin composite films of 0.90 mm thickness were obtained. The films were kept in desiccators at room temperature for at least 24 hours prior to examination. A Universal Testing Machine (UTM) was used to examine mechanical properties, such as tensile strength. The results of averaged measurements were presented after repeated measurements were taken to verify reproductivity.

Instrumental analysis

Different methods, including FT-infrared spectroscopy, UV-visible spectroscopy, P-XRD, SEM, SEM-EDX, TEM, CHN, TGA and DSC, were used to analyse the cellulose and lignin samples. To quantify the extent of crystallinity and other structural parameters that can help us understand different chemical, physical and mechanical properties, Fourier Transform Infrared (FTIR) spectra with a resolution of 4 cm^{-1} and in the range of 400-4000 cm^{-1} were recorded using a Perkin Elmer spectrophotometer (model Frontier MIR FIR) using the traditional KBr pellet method. Ultraviolet-visible (UV-visible) spectra were recorded for the solid phase, on a Shimadju UV-2550. A TGA 50, made by Shimadzu, Japan, was used to record thermal curves (TG/DTG), where 3–4 mg of sample was placed in a platinum crucible and heated to 600 °C at a rate of 20 °C per minute, while being exposed to dynamic nitrogen atmosphere flowing at a rate of 30 mL per minute. A Shimadzu DSC 60, Japan, was used to perform differential scanning calorimetry (DSC) between the temperatures of 50 and 100 °C, at a heating rate of 3 °C per minute, with a nitrogen flow rate of 30 mL per minute. The D8 Focus, Bruker AXS, Germany (Software XRD Commander 2, DIFFRAC.EVA; CuKα radiation with a wavelength of 1.541 Å (λ)) was used to conduct the powder X-ray diffraction (P-XRD) study at room temperature. A Perkin Elmer 2400 Series 2 (USA) was used to calculate the contents of C, H, and N. A JSM-6390LV SEM, JEOL software, Japan, was used to perform the SEM and EDX analyses of the samples. The TEM images were obtained on a TECNAI G2 20 S-TWIN, with a resolution of $2.4A^0$ (FEI Company, USA), and at an accelerating voltage of 200 kV; all the samples were centrifuged using a REMI R-8C centrifuge. The molecular weights and polydispersity indexes of both cellulose and lignin were determined by gel permeation chromatography analysis (UV/V Visible Detection-2489, Refractive Index Detector-2414, HPLC PUMP-515, Waters Corporation, USA, using Empower-2 software) using THF as solvent.

The hydrodynamic size and dynamic light scattering (DLS) measurements were ascertained using Micromeritics Nanoplus Zeta/Nano Particle Analyser by employing water as medium. With the aid of a 10 kN load cell and a 40 mm/min crosshead speed, the tensile strength was assessed using a Universal Testing Machine (UTM), Zwick Z010, Germany.

RESULTS AND DISCUSSION

Study on moisture content

As we know, when an object attracts moisture, it undergoes chemical, mechanical and biological decomposition reactions, especially the substances containing organic molecules. So, determining the moisture content and maintaining an optimum level is essential with the aim of preserving it. Therefore, it was quantitatively determined in both new and old cellulose fiber (NBC, OBC) and lignin (NBL, OBL). Both the extracted cellulose and lignin samples were stored in desiccators for about 3-4 weeks at standard room temperature of 25 °C, pressure of 760 mm Hg and relative humidity of 50% RH, prior to measuring the moisture content, so that equilibrium moisture content is achieved (Tappi T 550).

As seen in Figure 3, OBC revealed a higher moisture content percentage as compared to NBC, which might be due to the fact that cellulose, being a highly polar molecule due to the –OH groups present in glucose, and hydrophilic, tends to interact strongly with water.[33] This leads to a decrease in the mechanical properties, as several hydrogen bonds are lost and disrupted, by crosslinking with the hydroxyl groups on the cellulose chains, making it more easily deformed.[34] Similarly, OBL was seen to absorb more moisture compared to NBL. The hydrogen bonds present in lignin may be disrupted on interaction with water, resulting in reduced mechanical properties.[35] It can also be seen from the DLS measurements that new lignin was found to have a larger particle size, compared to old lignin, which was also confirmed by GPC analysis, as a result of which old lignin particles possessed a larger specific surface area and hence, higher moisture content due to greater absorption. The moisture content in cellulose and lignin can vary depending on the relative humidity (RH), where RH at a given temperature is defined as the ratio of partial pressure of vapor to the vapor pressure of water. It has been found that cellulose and lignin that had undergone some sort of oxidation over time resulted in a higher moisture uptake, which can be seen in the case of OBC and OBL.[36] Old cellulose had a higher moisture content, which might be due to the presence of a greater number of amorphous regions, as confirmed by XRD. Lignin is much more

vulnerable to oxidation than cellulose,[37] because of which we can see a higher difference in moisture content between NBL and OBL, as compared to NBC and OBC.

Evidence from UV-visible spectra

The UV−visible spectra of the cellulose and lignin samples were recorded in the wavelength range of 200−800 nm, as shown in Figure 4. The resonance forms of the groups in the cellulose molecule appear to absorb ultraviolet light in the energy range that is primarily between 200 and 300 nm.[38] A hypochromic effect is seen for OBC, as there is decreased absorption intensity, which might be due to distortion of the geometry of the molecules with ageing that results in decreased coplanarity, leading to loss of conjugation.[39] As regards MC, the introduced $ZrO_2.nH_2O$ might cause distortion of the geometry of molecules (amorphous nature of $ZrO_2.nH_2O$), resulting in poor conjugation or it might limit the resonance, which results in decreased absorbance.[40]

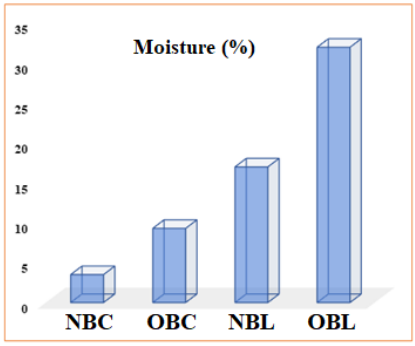

Figure 3: Moisture determination of cellulose and lignin

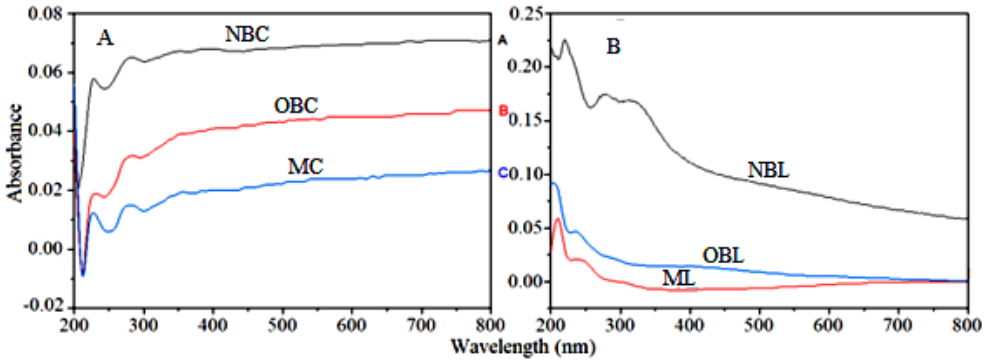

Figure 4: UV-visible spectra of (A) cellulose from new *Sānci* bark (NBC), old *Sānci* bark (OBC), modified cellulose (MC), and (B) lignin from new *Sānci* bark (NBL), old *Sānci* bark (OBL), modified lignin (ML)

UV spectroscopy refers to absorption spectroscopy in the UV wavelength region (200-400 nm), which has been used to record the spectrum of lignin, as shown in Figure 4.[41] Due to the aromatic nature of lignin, there is a strong absorption in the UV region. The aromatic ring's transition to the $\pi \rightarrow \pi^*$ state causes high absorption in the 200–220 nm region.[42] The absorption peaks of NL near 280-310 nm are due to the phenolic structure (benzene ring) substituted by hydroxyl or methoxyl groups.[42] The absorption band above 300 nm signifies the presence of conjugated structures present with aromatic moieties, while the absorption band in the visible region of the wavelength range from 400 nm to 600 nm is responsible for the dark brown colour of the extracted lignin.[43]

Similarly to cellulose, a hypochromic effect is also seen for OBL, as there is decreased absorption intensity, which might be due to distortion of the geometry of the molecules with ageing that results in decreased coplanarity, leading to loss of conjugation.[39] While for ML, the induced $ZrO_2.nH_2O$ might cause distortion of the geometry of molecules (amorphous nature of $ZrO_2.nH_2O$), resulting in poor conjugation or it might limit the resonance, which results in decreased absorbance.[40]

Evidence from FTIR spectra

From the FTIR spectra shown in Figure 5A, the broad peak absorption band at 3430 cm^{-1} for NBC and 3418 cm^{-1} for OBC is assigned to strong hydrogen bonded hydroxyl groups (–O–H) stretching generally observed in polysaccharides.[44] This peak includes also inter- and intra-molecular hydrogen bonds in NC and OBC. The stretching and deformation vibrations of the C-H group, typically seen in the glucose unit, are attributed to the bands at 2923 cm^{-1} and 1317 cm^{-1} for NBC, and at 2819 cm^{-1} and 1373 cm^{-1} for OBC.[45] The peaks located around 1633 cm^{-1} for both NBC and OBC correspond to vibration of water molecules absorbed in cellulose,[44] while the amorphous region is represented by the band at about 897 cm^{-1}.[44]

MC showed characteristic bands of cellulose, as reported earlier in this work and also agree with the values previously reported in literature.[46] The addition of ZrO_2 nanoparticles to our cellulose sample led to increased intensity of the O-H bond in the region around 3430 cm^{-1}.[47] This might be due to sorption of H_2O molecules on *Sānci* Cell/ZrO_2 surface, which became more hydrophilic due to polarity of Zr-OH. A slightly broader and stronger peak at around 3400 cm^{-1} can be observed in the case of OBC, which might be due to O-H in H_2O, as reported previously, meaning the OBC sample had absorbed more moisture from the atmosphere.

The first peak at 3434 cm^{-1} for NL and 3426 cm^{-1} for OBL can be attributed to the OH stretching vibration of the hydroxyl group, according to the FTIR spectra in Figure 5B.[48] Due to C-H stretching in the methyl and methylene group, the absorbance at 2920 cm^{-1} for NL and at 2936 cm^{-1} for OBL is caused.[49] At 2850 cm^{-1} for both NBL and OBL, a symmetric stretch for CH_3 of the methoxyl group was visible.[48] Ketone and carboxyl groups exhibit a peak at 1644 cm^{-1} for NBL and at 1652 cm^{-1} for OBL, which is attributed to carbonyl stretching.

The peaks at 1548 cm^{-1}, 1516 cm^{-1} and 1431 cm^{-1} for NL, and those at 1549 cm^{-1}, 1515 cm^{-1} and 1423 cm^{-1} for OBL are equivalent to aromatic skeletal vibrations, while for both NL and OBL the β-O-4 ether bond band was observed at 1124 cm^{-1}.[48] As seen in the cases of both the lignin and the primary alcohol, aromatic CH in-plane deformation, guaiacyl type, and C-O stretching may be the causes of a small peak around 1030 cm^{-1}.[48] The aromatic and aliphatic hydroxyl groups in the lignin samples showed O-H stretching, which produced a strong and broad absorption band between 3600 and 3200 cm^{-1}.[49]

The modification also showed an increase in the hydrophilic nature of the lignin, because the ratio of the C-H stretching band intensity (2920 cm^{-1}) is lower in the spectrum of the *Sānci* Lig/ZrO2.nH2O material than that observed for the pure lignin. Moreover, the FTIR spectra of NBL and OBL samples almost overlap, meaning the structural and chemical composition of both samples are almost identical. This is because lignin has a complex structure that is challenging to break down. Ether linkages and carbon-carbon bonds, which hold the lignin units together, are compelling and stable bonds.

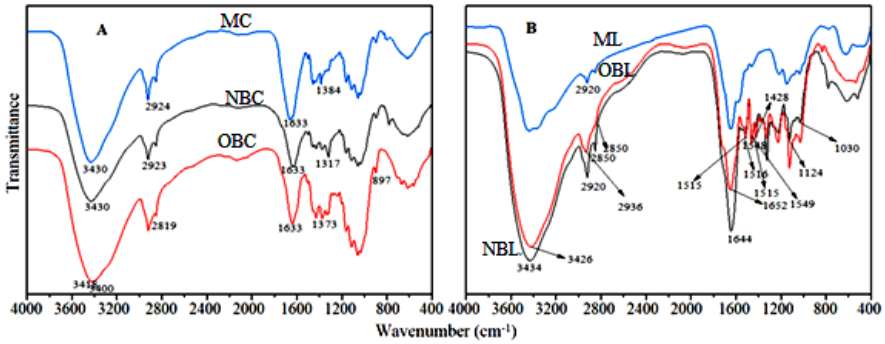

Figure 5: FTIR spectra of (A) cellulose from new Sānci bark (NBC), old Sānci bark (OBC), modified cellulose (MC), and (B) lignin from new Sānci bark (NBL), old Sānci bark (OBL), modified lignin (ML)

Evidence from TGA-DTG spectra

Thermogravimetric spectra of all cellulose and lignin samples are shown in Figure 6. The two weight loss stages of thermal decomposition of the cellulose fibers correspond to the slow pyrolysis and fast pyrolysis stages. Weight loss was connected to the volatilization and vaporization of absorbed water molecules, as well as the removal of moisture content at the early and slow pyrolysis stage of the curve between 30

°C and 160 °C for NBC, 30 °C to 180 °C for OBC, and 30 °C to 190 °C for MC. Fast pyrolysis occurred between 265 °C to 360 °C for NBC, 256 °C to 380 °C for OBC and 250 °C to 390 °C for MC, as shown by the broad peaks on the DTG curves. Due to the cellulose's decomposition and dehydration, the weight loss occurred relatively quickly. Because of oxidative thermal degradation, and depolymerization of the cellulose chain, cellulose was almost completely burned during this stage. Nearly all of the cellulose was pyrolyzed at temperatures above 400 °C, leaving only a minimal amount of solid residue. Maximum degradation occurred at 317 °C for NBC, 338 °C for OBC and 320 °C for MC, as shown in the DTG curves.

Between the different samples of cellulose, MC and OBC underwent the maximum weight loss in the first stage due to removal of moisture. This might be explained by the fact that, after modification, there is an increase in the hydrophilic character of the fibers, while for OBC, it might be due to prolonged exposure to the atmosphere over a very long period of time. The highest weight loss was seen in cellulose (old), which may be related to lower intermolecular van der Waals forces and hydrogen bonding, although a similar thermal degradation and a corresponding percentage weight loss were observed in cellulose samples.[50]

Compared to cellulose, lignin decomposes more slowly and over a wider temperature range because of its complex structure and composition. This is because different oxygen functional groups from lignin's structure have different thermal stabilities and scission occurs at various temperatures.[51] As seen up to 120 °C for NBL, 110 °C for OBL, and 130 °C for ML, free and bound water evaporated, which resulted in the lignin samples losing weight. For NBL, OBL, and ML, the moisture removal or drying stage is defined as a weight loss of approximately 0.3%, 1%, and 0.4%, respectively. Disappearance of side chains, releasing volatiles like CH_4, CO, CO_2, *etc*., is the cause of the shoulder-like peaks in the lignin samples on the DTG curve in the temperature ranges of 120–200 °C. The DTG curve's broad peaks show that the lignin samples quickly degraded through pyrolysis in the temperature range of 220–515 °C for NL, 200–510 °C for OBL, and 230–600 °C for ML. The primary pyrolysis stage is considered to have occurred at this point, because the lignin sample had lost most of its initial weight.

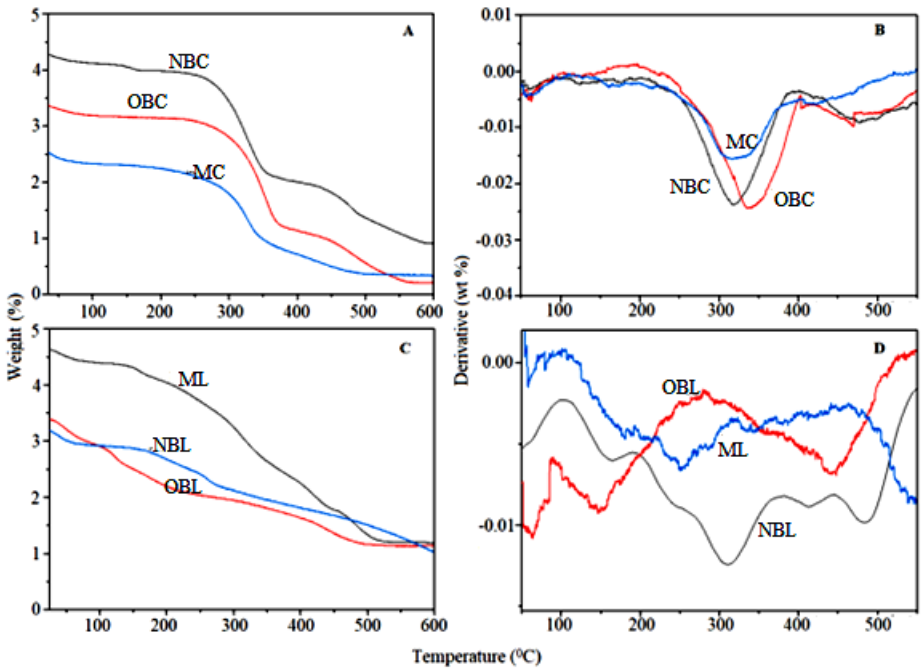

Figure 6: TG patterns of (A) cellulose from old Sānci bark (OBC), new Sānci bark (NBC), modified cellulose (MC); DTG patterns of (B) cellulose from old Sānci bark (OBC), new Sānci bark (NBC), modified cellulose; (C) lignin from old Sānci bark (OBL), new Sānci bark (NBL), modified lignin (ML); (D) lignin from old Sānci bark (OBL), new Sānci bark (NBL), modified lignin (ML)

The interunit linkages are broken down during the pyrolytic degradation process, which release vaporization of monomeric phenols and their derivatives. Maximum degradation occurred at 310 °C for NBL, 400 °C for OBL, and 560 °C for ML, as shown in the DTG patterns, which exhibit wide and flat peaks. Due to its complex composition and structure, it is difficult to ascertain with clarity as to why the different lignin samples possess variable maximum degradation temperatures. Moreover, the thermal degradation of lignin is strongly influenced by its nature and moisture content, reaction temperature and degradation atmosphere, heat and mass transfer processes, and as such, more studies are required to completely understand this phenomenon.[52] Among the different samples of lignin, OBL underwent the maximum weight loss in the first stage due to removal of moisture. It might be due to the prolonged exposure to the atmosphere over a lengthy period of time. Although all the lignin samples had a similar course of thermal degradation and corresponding percentage weight loss, the DTG of OBL was higher than that of NBL, and modified lignin had the highest DTG of all the lignin samples. It is thermally more stable because the DTG value is higher. OBL may have higher thermal stability than NBL, because it contains more C-C linkages and aromatic moieties, which are very stable and require a higher temperature to fragment. As for modified lignin, it is thermally the most stable, which might be due to ZrO_2, a derivative of zirconium oxychloride, that is induced in the modified lignin, which exhibits excellent thermal stability and also may be due to the cleavage of the aryl–ether linkages, resulting in stable intermediate products.[53]

Evidence from DSC spectra

The thermal stability of cellulose and lignin assessed through DSC analysis is shown in Figure 7. The heat of reaction is measured in between 0 °C and 300 °C. From 60 °C to 100 °C for NBC, 50 °C to 80 °C for OBC, and 65 °C to 120 °C for MC, the first endotherm of cellulose began. It is believed that these endotherm transitional ranges correspond to an amorphous component that led to the rearrangement of the molecular chains, according to Nandanwar *et al.*[48] This small change in enthalpy may also be caused by the desorption of moisture, as water trapped in the polysaccharide structure is released. The second endothermic transition, which corresponds to the cellulose crystallite portion, was visible for NBC, OBC, and MC between 180 °C and 200 °C, whereas it was visible for MC between 200 °C and 210 °C. This endothermic transition was attributed to the onset of cellulose thermal degradation, which includes molecular chain rearrangement, glycosidic bond cleavage, intermolecular cross-linking, and finally cellulose depolymerization, involving the dissolution of intramolecular interactions.[50]

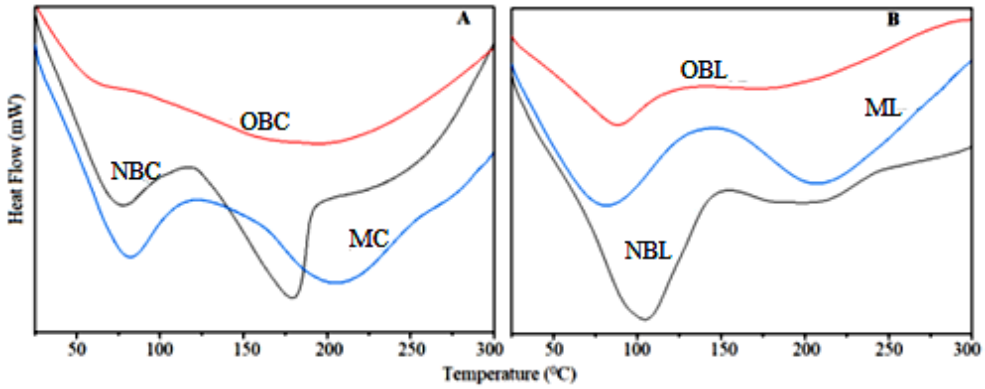

Figure 7: DSC spectra of (A) cellulose from old Sānci bark (OBC), new Sānci bark (NBC), modified cellulose (MC); (B) lignin from old Sānci bark (OBL), new Sānci bark (NBL), modified lignin (ML)

A very large and broad peak was observed for the endothermic transition in the case of OBC due to moisture loss in our sample, along with the fact that OBC having a lower crystallinity index, contains more amorphous regions. So, it consists of a range of interactions and thereby softens gradually. The second endothermic peak for modified cellulose slightly shifted to higher temperature, which may be due to the presence of zirconium oxide nanoparticles.[49]

DSC is regarded as a top-notch thermo-analytical technique for determining the glass

transition temperature (Tg) of amorphous polymers like lignin. The DSC heating curve shows a slight change in baseline rather than a sharp peak during this process, because the glass transition of lignin is not a known phase.[49] As a result, the small variations on the DSC baseline at 140 °C, 130 °C, and 110 °C were identified as the Tg for NBL, OBL, and ML, respectively. The lower Tg value of OBL suggests that its main chain is more pliable and less rigid, which allows for rotation at lower temperatures. Due to its less compact nature, it may also imply that OBL has fewer intermolecular interactions. This structural characteristic of OBL also suggests that it has the additional ability to create monomers physically linked together. Below the glass transition temperature (Tg), the polymer becomes glassy, and above which, it becomes rubbery (soft) and dimensional stability is lost.

After modification, the lignin sample showed the lowest Tg value, which can be related to a more flexible chain structure, lower intermolecular forces of interactions and enhanced presence of cross-linking between the monomers. Identifying the Tg of polymers is often used for better conceiving the potential applications of such polymers, and thus it represents a key step in commercial polymer research and development. The endothermic peaks at 220 °C, 225 °C and 235 °C on the DSC curves for NBL, OBL and ML, respectively, might be due to lignin going through a complex reaction, including endothermic, obvious volume expansion and microscopic surface change.[54] It might also be caused by a lignin network cracking reaction with formation of volatile substance.[55] Overall, the degradation of lignin occurs at a higher temperature because of hydrogen bonds between the –OH of the phenolic groups of lignin. The endothermic peaks of NBL and OBL are at temperatures very close to each other, which might be due to its complex composition and structure, as well as higher crosslinking.[56] Modified lignin, on the other hand, is deemed to have higher thermal stability and the side chains will not fragment easily to release volatiles.

Evidence from CHN analysis

Table 1 shows different elemental composition percentage of C, H and N in cellulose and lignin samples extracted from *Sānci* bark. The high carbon content might have played a role in maintaining the structural integrity of cellulose. Cellulose samples did not contain nitrogen, which might have helped in slowing down the rate of decomposition by fungi, actinomycetes, and bacteria. A slight increase in nitrogen content was also seen after contact with nitrogen containing solvents or chemicals in the lab, such as urea in this case, which had been used to prepare the zirconium modified cellulose sample.

For lignin, lower carbon content was seen in the modified sample, which might be due to Zr nanoparticles being incorporated in between the lignin matrix, while nitrogen content also increased after the treatment with urea. The origin of nitrogen in lignin samples is from cell proteins. It is believed that the complexity of its bonds, the presence of cross-linkages in its structure, and the relatively low nitrogen content of lignin all contribute to the slow rate of decomposition of lignin by fungi, actinomycetes, bacteria, *etc*.[57]

Table 1
CHN analysis of cellulose and lignin

Sample	C (%)	H (%)	N (%)
Old cellulose	37.29	6.12	0.06
New cellulose	39.5	5.49	0
Modified cellulose	34.21	5.47	1.78
Old lignin	31.54	6	2.45
New lignin	30.99	4.89	2.61
Modified lignin	29.22	5.21	7.73

Evidence from SEM images

SEM images of all the cellulose and lignin samples are shown in Figure 8. The new cellulose image is quite brighter than that of the old one. The lignin samples appear to have a cylindrical shape, where OBL shows many open volumes, which might be due to the lignin extraction process. Figure 10 reveals a considerable number of fine particles or flakes deposited on the surface of cellulose and lignin fibers heterogeneously, which confirms the presence of $ZrO_2.nH_2O$ nanoparticles. This heterogeneity may occur

because of the lack of agitation. Also, roughness on the surface is observed.

Evidence from EDXA spectra

From the EDXA spectra (Fig. 9), it is clearly seen that the carbon content is slightly higher in the case of both OBC and OBL, in comparison with NBC and NL. However, oxygen is slightly higher in the case of NBC and NBL. EDXA spectra also confirmed that zirconium oxychloride nanoparticles were successfully incorporated into MC and ML.

Evidence from TEM images

As seen from Figure 10, $ZrO_2.nH_2O$ nanoparticles were successfully incorporated in the cellulose and lignin samples, heterogeneously, because of different particle sizes. Also, the nanoparticles show agglomeration because of their small particle size. On the surface of the cellulose, heterogeneous deposition of $ZrO_2.nH_2O$ nanoparticles was observed, with diameters of 50 to 75 nm, and on the lignin – with diameters of 40 to 60 nm.

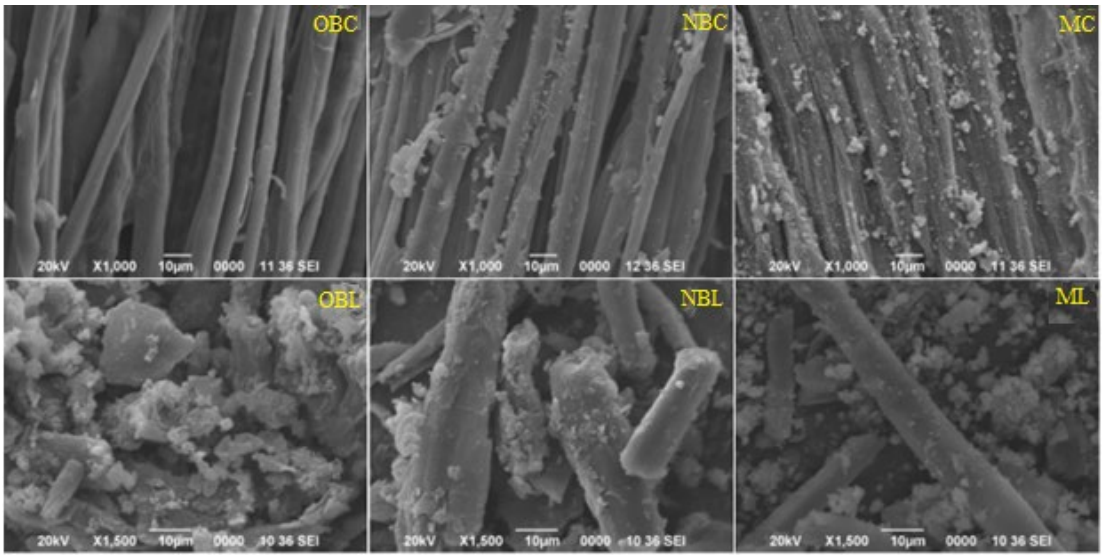

Figure 8: SEM images of cellulose from old Sānci bark (OBC), new Sānci bark (NBC), modified cellulose (MC); lignin from old Sānci bark (OBL), new Sānci bark (NBL), modified lignin (ML)

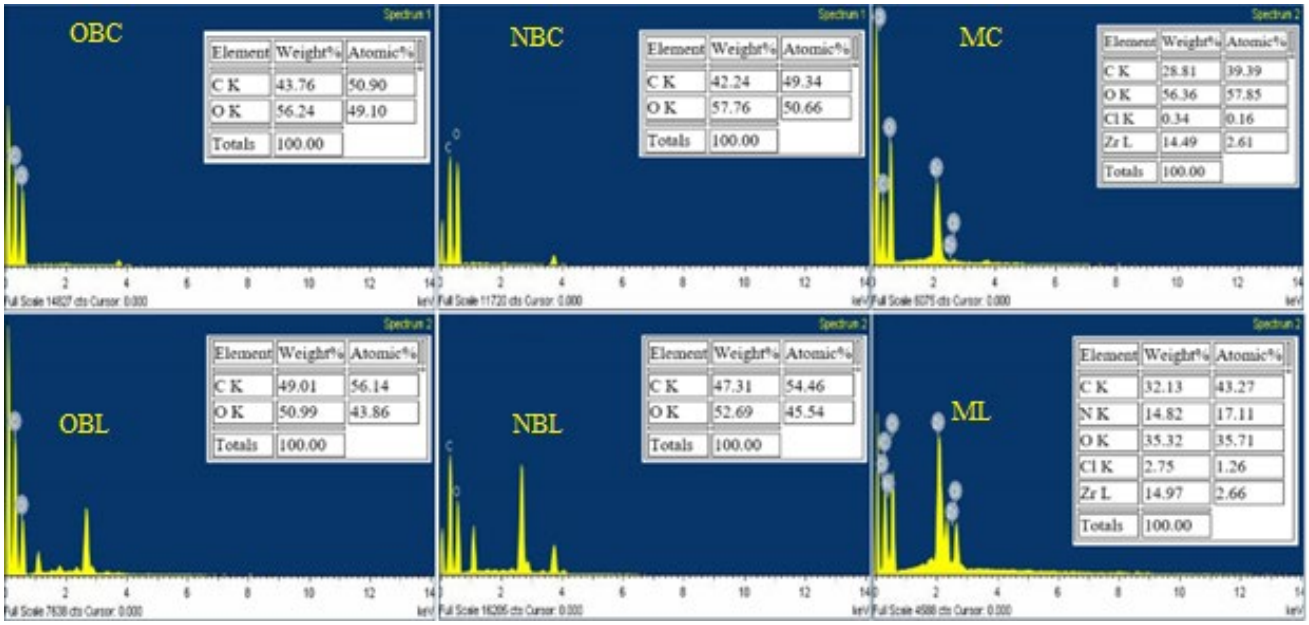

Figure 9: EDXA spectra of cellulose from old Sānci bark (OBC), new Sānci bark (NBC), modified cellulose (MC); lignin from old Sānci bark (OBL), new Sānci bark (NBL), modified lignin (ML)

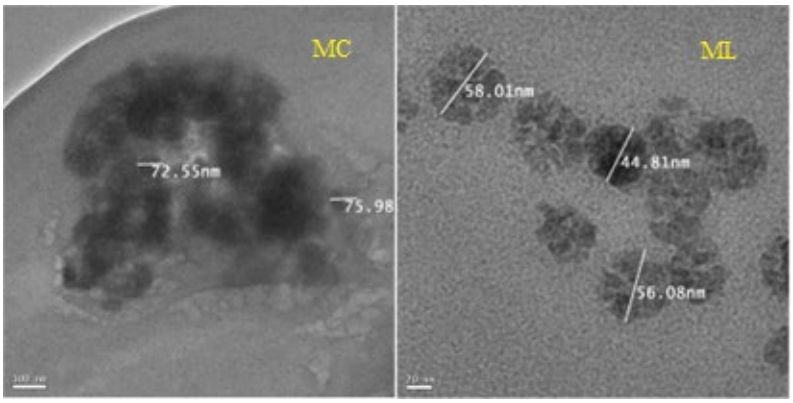

Figure 10: TEM images of modified cellulose (MC) and modified lignin (ML)

Evidence from p-XRD spectra

All the 2θ values in the p-XRD spectra are obtained from CuKα radiation with a wavelength of 1.541Å (λ). The diffraction patterns of cellulose and lignin are shown in Figure 11.[58-60] Peak deconvolution has been performed using the Lorentzian function ranging 2θ from 10° to 40° to determine the relative contributions of each peak to the crystallographic planes of (1-10), (110), (020), *etc*.[58-62] (Fig. 12).

The p-XRD spectra of NC showed the characteristic peaks of cellulose Iβ, where the main contributors of intensity to the three diffraction peaks have Miller indices of crystallographic planes (1-10), (110) and (020) at 2θ values of 14.5°, 16.97° and 22.3°, respectively.[58,62-64] Because of the severe peak overlap of several reflections in the region near 34.5°, it was difficult to correctly estimate the (004) signal.[63] Other reflections obtained are not considered as dominant contributors. For OBC, peak deconvolution was carried out using the same method as described above, and characteristic peaks for cellulose Iβ are shown. A slight shift in the peaks (by 1°) can be seen in the case of OBC for some of the crystallographic planes. This might be due to the change in lattice parameters (either lattice expansion or contraction) like crystallite size, lattice strain, *etc*., which can occur with ageing and degradation.[65] The MC patterns are amorphous due to modification of the cellulose with zirconium oxide.[21] The X-ray diffractograms for cellulose modified by precipitation with zirconium oxide nanoparticles completely lose their reflections specific to the crystalline organization because of the amorphous character of $ZrO_2.nH_2O$ and also due to generation of disorder when the fibers are modified.[30]

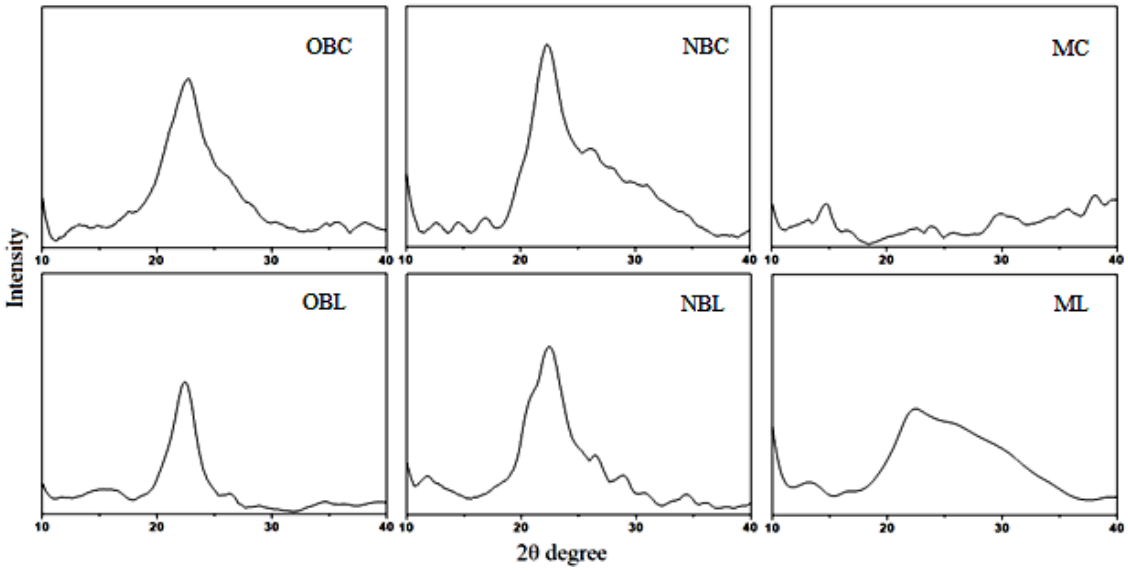

Figure 11: p-XRD spectra of cellulose from old Sānci bark (OBC), new Sānci bark (NBC), modified cellulose (MC); lignin from old Sānci bark (OBL), new Sānci bark (NBL), modified lignin (ML)

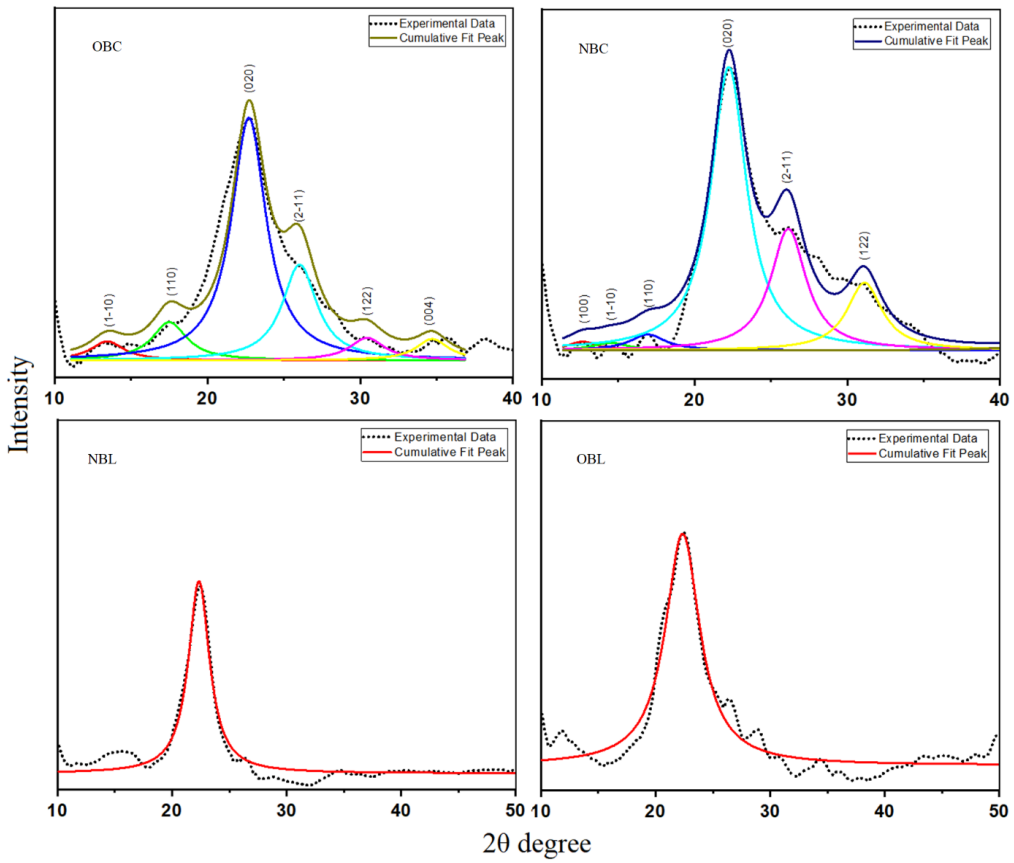

Figure 12: X-ray diffraction patterns of cellulose from old Sānci bark (OBC) and new Sānci bark (NBC); lignin from old Sānci bark (OBL) and new Sānci bark (NBL)

Table 2
Band position (2θ) and d-spacing of NBC

	(1-10)	(110)	(020)
2θ	14.6114	16.9381	22.6564
d (A^0)	3.0543	2.6446	2.0002

Specific reflections of the nano zirconium oxide did not appear in the X-ray diffractograms for the modified cellulose and lignin, unlike the results for modified cellulose fibers from sugarcane bagasse reported by Mulinary *et al.*[21] Further studies will be interesting to get a better understanding of how the nanoparticles interact with these types of cellulose fibers and lignin extracted from tree barks.

Interplanar spacing (d-spacing) for NC crystallographic planes was calculated from Bragg's equation, $n\lambda = 2d\sin\theta$, as shown in Table 2.[66]

The monoclinic or triclinic structure of cellulose was determined as per the method developed by Wada *et al.*[66] Discriminant analysis was done according to Samuel *et al.* to categorize NBC into Iα or Iβ predominant form. The function that decides whether it is a monoclinic or triclinic structure is $Z = 1693d_1 - 902d_2 - 549$,[64] where d_1(nm) is the d-spacing of the Iβ (1-10) peak and d_2(nm) is the d-spacing of the I_β (110) peak. $Z > 0$ indicates that the extracted cellulose is rich in the Iα form, while $Z < 0$ indicates that I_β is the predominant form in the sample. The Z values of the NBC sample obtained were found to be less than zero, suggesting that the sample belonged to the Iβ form (dominant monoclinic structure).

For both NBL and OBL, peak fitting was carried out using the Lorentzian function as the Lorentzian character is more prominent in hardwood samples. After fitting the curves, NBL and OBL diffraction peaks were located at 2θ of 22.33^0.[67] Kubo *et al.* reported the diffraction angle 2θ of 22.7^0 for hardwood acetic acid lignin, and Ansari and Gaikar reported 2θ of 22.37^0 for lignin from sugarcane bagasse.[68,69] Such small

differences may be caused by the difference in the lignin type, being obtained from different sources. The ML patterns are amorphous due to modification of the cellulose with zirconium oxide.

Evidence from GPC analysis

A popular and widely accepted technique for determining the molecular weights (MW), molecular weight distributions (MWD), and polydispersity indices (PDI) of polymers is gel permeation chromatography (GPC). Samples of lignin were not totally dissolved in tetrahydrofuran (THF) even after stirring and sonication, so the soluble fraction after filtration through the Teflon membrane with a pore size 0.45 μm was analyzed by GPC.[70]

Pure cellulose fiber, extracted from *Sānci*, could not be investigated by GPC as it is insoluble in the standard eluent tetrahydrofuran due to its high molecular weight. Table 3 displays the polydispersity index (PDI) values, number average and weight average molecular weights (Mn and Mw), and molecular weights for the lignin samples. PDI values of all the lignin samples are nearly equivalent to one, as expected, since lignin is a natural polymer. Slightly higher molecular weight distribution was observed for NBL resulting in better mechanical properties.[71] However, the difference in molecular weight distribution between NBL and OBL was not that significant, implying that the structural integrity of lignin even after ageing was more or less intact due to its complex structure. ML was seen to have a lower molecular weight distribution, which might be due to chain scission and ring opening caused by the modification, thereby resulting in increased chain mobility and a less compact structure. Since NBL sample has been recorded as having slightly higher average molecular weight than that of OBL, it may be concluded that the NBL has a higher average particle size, as a higher PDI value also corresponds to a larger particle size distribution in the sample.[72]

Table 3
Molecular weight distribution and polydispersity of lignin samples

Sample	M_n	M_w	Polydispersity
New lignin	1414	1500	1.06
Old lignin	1416	1448	1.02
Modified lignin	1262	1330	1.05

Evidence from dynamic light scattering (DLS) analysis

DLS is a useful technique for studying particle size distribution – the light scattered by the particles in suspension fluctuates over time, which can be related to the particle diameter.[73] For DLS measurements, lignin samples were dispersed in water for 2 days by sonication. Table 4 lists the particle size diameter of lignin samples, including D_{10} (10% of the total of particles lie below this diameter), D_{50} (50% of the total of particles lie below this diameter), D_{90} (90% of the total of particles lie below this diameter), and D_{av} (average diameter of particles). Figure 13 displays the DLS spectra. The average diameter of NBL, OBL and ML particles was found to be 1.72 μm, 1.24 μm and 4.87 μm, respectively. NBL was found to have a larger particle size, compared to OBL, as also confirmed by GPC analysis. Decreasing particle size in the case of OL might be due to the various degradation processes that take place over time, which results in an increase in viscosity and the surface area for more reactions to occur. Decreasing size of particles also leads to lower crystallinity, as seen in P-XRD analysis for OBL.[74] While modified lignin had the largest particle size among all of them, due to zirconium nanoparticles being introduced within the lignin matrix, which caused agglomeration, thereby resulting in an increase in the diameter.

Investigation of mechanical properties by UTM

The PVA films, PVA/Cellulose composite films and PVA/Lignin composite films were cast on 150 mm x 15 mm standard round Petri dishes and had lengths of 35 mm and an area of 19.635 cm^2. The UTM measurements were carried out as per ASTM D368 using a 5 min/mm crosshead speed and were repeated thrice for reproducibility. PVA films were used as reference and the tensile strength of the film was found to be 2.24 MPa from UTM measurements. An increase in tensile strength was observed for the PVA/Cellulose and PVA/Lignin composite films, as compared to the PVA film. This demonstrates that cellulose fibers

and PVA, as well as lignin and PVA are highly compatible.

Table 4
Particle size of different lignin samples

Sample	Particle diameter	Size (μm)
New lignin	D_{10}	0.43
	D_{50}	1.31
	D_{90}	6.08
	$D_{average}$	1.72
Old lignin	D_{10}	0.36
	D_{50}	1.49
	D_{90}	6.65
	$D_{average}$	1.24
Modified lignin	D_{10}	1.73
	D_{50}	4.66
	D_{90}	13.30
	$D_{average}$	4.87

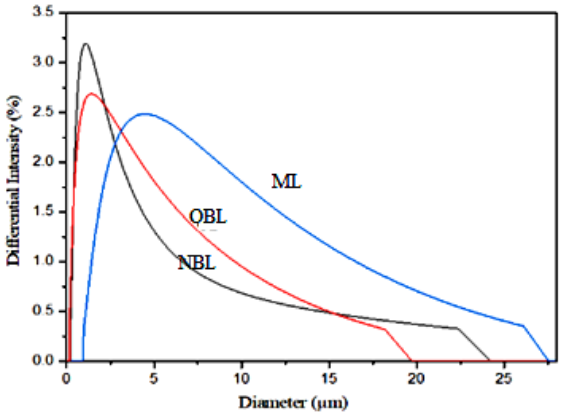

Figure 13: DLS size distribution spectra of lignin from old Sānci bark (OBL), new Sānci bark (NBL) and modified lignin (ML)

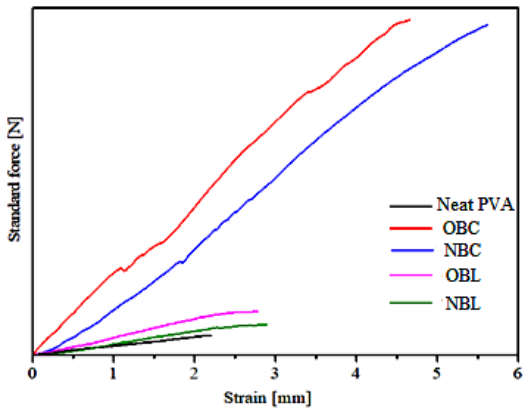

Figure 14: Mechanical strength analysis by UTM of neat PVA, PVA/old bark cellulose (OBC), PVA/new bark cellulose (NBC), PVA/old bark lignin (OBL) and PVA/new bark lignin (NBL) film

Table 5
Tensile strength of different cellulose and lignin film along with PVA

Sample	Tensile strength (MPa)	Mean tensile strength (MPa)	Standard deviation
PVA	2.24 0.88 1.02	1.38	0.74
Old cellulose	4.66 3.21 5.98	4.61	1.38
New cellulose	5.61 5.02 6.62	5.75	0.81
Old lignin	2.87 2.32 1.99	2.39	0.44
New lignin	3.02 2.25 2.09	2.45	0.49

The enhanced tensile strength properties of the PVA/Cellulose and PVA/Lignin composites, compared to PVA, and, consequently, the intense reinforcing action of cellulose and lignin, may be explained by strong intermolecular hydrogen bonding between the hydroxyl groups of cellulose, lignin, and the PVA matrix.[75]

The results of the mechanical analysis of tensile strengths of different PVA/Cellulose and PVA/Lignin films are summarized in Table 5 and representative stress-strain curves are shown in Figure 14. A clear decrease in the tensile strength of the PVA-OBC film was observed, which could be correlated with the higher moisture content seen in the case of OBC. As the strength of the cellulose decreases, the chains loosen and become less compact because of poor intermolecular interactions.[76] Also, absorbed water in a polymer behaves like a plasticizer, which reduces the entanglement and bonding between molecules, affecting various mechanical properties.[77]

Similarly, the tensile strength decreases for the PVA-OBL film, which could be correlated with the lesser extent of hydrogen bond formation between OBL and PVA, as result of which the intermolecular interactions decrease and chain entanglement lowers, resulting in a flexible structure.[76] Further analysis of PVA/Cellulose and PVA/Lignin blends using FT-IR is necessary to better understand the intermolecular interactions occurring between the components. However, the decrease in tensile strength was much more prominent in the case of the PVA/Cellulose samples, as compared to the PVA/Lignin samples. This could be due to the complex and highly branched structure of lignin, which contains both aliphatic and aromatic residues that do not degrade easily with ageing.[78]

CONCLUSION

Cellulose and lignin were extracted from a century old and new *Sānci* bark using alkaline and peroxide treatments for cellulose and acidic treatments for lignin. The cellulose and lignin extracted from new *Sānci* bark were embedded with $ZrO_2.nH_2O$ nanoparticles using zirconium oxychloride. Old cellulose (OBC) and old lignin (OBL) were found to show a higher moisture content percentage, compared to new cellulose (NBC) and new lignin (NBL), reducing mechanical properties in both OBC and OBL. The structural and chemical compositions were nearly identical, indicating only minor degradation of the intricate structure. The complex composition and structure of lignin result in a slower thermal decomposition rate. It can withstand a wider range of temperatures, compared to cellulose, because the different oxygen functional groups that make up its structure have different thermal stabilities and scission temperatures. The cellulose samples were found to have high carbon content, which is an excellent property due to its good chemical and weathering resistance. The carbon content is marginally higher for both OBC and OBL, compared to NBC and NBL. Heterogeneous deposition of $ZrO_2.nH_2O$ nanoparticles on cellulose and lignin was observed.

Better mechanical properties of NBC have been observed. A lower level of mechanical strength for OBC is seen because of aging and degradation. The amorphous nature of $ZrO_2.nH_2O$ may cause the gradual reduction in XRD peak intensity observed for MC and ML. OBL particles had the least average diameter among NBL, OBL, and ML particles. The P-XRD of OBL confirmed that, as particle size decreases, mechanical strength also decreases. The apparent decrease in tensile strength of PVA-OBC and PVA-OBL films was noticed. This finding could be related to the higher moisture content found in OBC and OBL. Zirconium oxychloride modifications in the case of NBC and NBL should not affect the conservation of heritage manuscripts.

ACKNOWLEDGMENT: A.A.A. thanks Tezpur University for an Innovation Research Grant and an Institutional fellowship. The authors also thank SAIC, Tezpur University, for providing instrumentation facilities.

REFERENCES

[1] *Ø*. Ellefsen and N. Norman, *J. Polym. Sci*., **58**, 769 (1962), https://doi.org/10.1002/pol.1962.1205816647

[2] S. B. Mishra, A. Mishra, N. Kaushik and M. A. Khan, *J. Mat. Process. Tech*., **183**, 273 (2007), https://doi.org/10.1016/j.jmatprotec.2006.10.016

[3] R.-L. Wu, X.-L. Wang, F. Li, H.-Z. Li and Y.-Z. Wang, *Bioresour. Technol*., **100**, 2569 (2009), https://doi.org/10.1016/j.biortech.2008.11.044

[4] Y.-L. Chung, J. V. Olsson, R. J. Li, C. W. Frank, R. M. Waymouth *et al*., *ACS Sust. Chem. Eng*., **1**, 1231 (2013), https://doi.org/10.1021/sc4000835

[5] O. Gordobil, R. Moriana, L. Zhang, J. Labidi and O. Sevastyanova, *Ind. Crop. Prod*., **83**, 155 (2016), https://doi.org/10.1016/j.indcrop.2015.12.048

[6] H. Chen, "Biotechnology of Lignocellulose: Theory and Practice", Springer, 2014, pp. 25-71, https://doi.org/10.1007/978-94-007-6898-7

[7] J. Strnadová and M. Ďurovič, *Restaurator*, **15,** 220 (1994), https://doi.org/10.1515/rest.1994.15.4.220
[8] V. Daniels, in *Science*, *Technology and European Cultural Heritage*: *Proceedings of the European Symposium*, Bologna, Italy, 13-16 June 1989, Butterworth-Heinemann Publishers, Oxford, 1991, pp. 269
[9] D. Klemm, B. Philpp, T. Heinze, U. Heinze and W. Wagenknecht, "Comprehensive Cellulose Chemistry. Volume 1: Fundamentals and Analytical Methods", Wiley-VCH Verlag GmbH, 1998
[10] I. Haq, P. Mazumder and A. S. Kalamdhad, *Bioresour*. *Technol*., **312**, 123636 (2020)
[11] S. M. Notley and M. Norgren, *Langmuir*, **26**, 5484 (2010), https://doi.org/10.1021/la1003337
[12] R. B. Santos, P. Hart, H. Jameel and H.-M. Chang, *BioResources*, **8**, 1456 (2013)
[13] H. Erdtman, in "Lignins: Occurrence, Formation, Structure and Reactions", edited by K. V. Sarkanen and C. H. Ludwig, New York, John Wiley Sons Inc., 1972, https://doi.org/10.1002/pol.1972.110100315
[14] C. Crestini, F. Melone, M. Sette and R. Saladino, *Biomacromolecules*, **12**, 3928 (2011), https://doi.org/10.1021/bm200948r
[15] E. Sjostrom, "Wood Chemistry: Fundamentals and Applications", Gulf professional publishing, 1993
[16] J. J. Liao, N. H. Abd Latif, D. Trache, N. Brosse and M. H. Hussin, *Int*. *J*. *Biol*. *Macromol*., **162**, 985 (2020), https://doi.org/10.1016/j.ijbiomac.2020.06.168
[17] S. Kalia, "Biodegradable Green Composites", John Wiley & Sons, 2016
[18] S. Zervos, in "Cellulose: Structure and Properties, Derivatives and Industrial Uses", edited by A. Lejeune and T. Deprez, Nova Publishing, 2010, pp. 155-203
[19] A. A. Ali, B. R. Goswami, N. Ligira and R. K. Dutta, *Curr*. *Sci*., **123**, 1359 (2022)
[20] R. K. Dutta, in "Religious Traditions and Social Practices in Assam", edited by D. Nath, DVS Publication, 2015, pp. 239-261
[21] D. Mulinari, T. Cruz, M. Cioffi, H. J. C. Voorwald, M. Da Silva *et al*., *Carbohyd*. *Res*., **345**, 1865 (2010), https://doi.org/10.1016/j.carres.2010.05.011
[22] G. Goncalves, P. A. Marques, R. J. Pinto, T. Trindade and C. P. Neto, *Compos*. *Sci*. *Tech*., **69**, 1051 (2009), https://doi.org/10.1016/j.compscitech.2009.01.020
[23] R. J. Pinto, P. A. Marques, A. M. Barros-Timmons, T. Trindade and C. P. Neto, *Compos*. *Sci*. *Tech*., **68**, 1088 (2008), https://doi.org/10.1016/j.compscitech.2007.03.001
[24] F. A. Pavan, M. S. P. Francisco, R. Landers and Y. Gushikem, *J*. *Brazil*. *Chem*. *Soc*., **16**, 815 (2005), https://dx.doi.org/10.1590/S0103-50532005000500021
[25] E. A. Toledo, Y. Gushikem and S. C. de Castro, *J*. *Colloid*. *Interface*. *Sci*., **225**, 455 (2000), https://doi.org/10.1006/jcis.2000.6767
[26] M. Sain and J. Boucher, *Colloid*. *Surface A*: *Phys*. *Eng*. *Asp*., **196**, 97 (2002), https://doi.org/10.1016/S0927-7757(01)00815-9
[27] E. A. Campos and Y. Gushikem, *J*. *Colloid*. *Interface*. *Sci*., **193**, 121 (1997), https://doi.org/10.1006/jcis.1997.5051
[28] A. Ajith, G. Xian, H. Li, Z. Sherief and S. Thomas, *J*. *Compos*. *Mater*., **50**, 627 (2016)
[29] M. Barathi, A. S. K. Kumar and N. Rajesh, *Ultrason*. *Sonochem*., **21**, 1090 (2014), https://doi.org/10.1016/j.ultsonch.2013.11.023
[30] G. A. Martins, P. H. F. Pereira and D. R. Mulinari, *BioResources*, **8**, 6373 (2013)
[31] N. Fitriana, A. Suwanto, T. Jatmiko, S. Mursiti and D. Prasetyo, *IOP Conf*. *Series*: *Earth Environ*. *Sci*., **462**, 012053 (2020), https://doi.org/10.1088/1755-1315/462/1/012053
[32] D. Suryawanshi, P. Sinha and O. Agrawal, *Restaurator*, **15**, 65-78 (1994).
[33] L. Lim and L. S. Wan, *Drug Devel*. *Ind*. *Pharm*., **20**, 1007 (1994), https://doi.org/10.3109/03639049409038347
[34] A. N. Frone, D. M. Panaitescu, D. Donescu, C. Radovici, M. Ghiurea *et al*., *Mater*. *Plast*., **48**, 138 (2011), https://revmaterialeplastice.ro/pdf/FRONE%20A.pdf%202%2011.pdf
[35] P. Posoknistakul, C. Tangkrakul, P. Chaosuanphae, S. Deepentham, W. Techasawong *et al*., *ACS Omega*, **5**, 20976 (2020), https://pubs.acs.org/doi/pdf/10.1021/acsomega.0c02443
[36] M. Garg, V. Apostolopoulou-Kalkavoura, M. Linares, T. Kaldéus, E. Malmström *et al*., *Cellulose*, **28**, 9007 (2021), https://doi.org/10.1007/s10570-021-04099-9
[37] E. Małachowska, M. Dubowik, P. Boruszewski, J. Łojewska and P. Przybysz, *Sci*. *Rep*., **10**, 19998 (2020), https://doi.org/10.1038/s41598-020-77101-2
[38] B. Lindman, G. Karlström and L. Stigsson, *J*. *Mol*. *Liq*., **156**, 76 (2010), https://doi.org/10.1016/j.molliq.2010.04.016
[39] U. P. Agarwal, S. A. Ralph, C. Baez, R. S. Reiner and S. P. Verrill, *Cellulose*, **24**, 1971 (2017), https://doi.org/10.1007/s10570-017-1259-0
[40] Z. Jiang, J. Yi, J. Li, T. He and C. Hu, *ChemSusChem*, **8**, 1901 (2015)
[41] J. W. Rowen, C. M. Hunt and E. K. Plyler, *Text*. *Res*. *J*., **17**, 504 (1947), https://doi.org/10.1177/004051754701700905
[42] Y. Li, L. Xue, H. Li, Z. Li, B. Xu *et al*., *Macromolecules*, **42**, 4491 (2009), https://doi.org/10.1021/ma900623p
[43] Y. Li and Y. Zou, *Adv*. *Mater*., **20**, 2952 (2008), https://doi.org/10.1002/adma.200800606
[44] W. Wu, T. Liu, X. Deng, Q. Sun, X. Cao *et al*., *Int*. *J*. *Biol*. *Macromol*., **126**, 1030 (2019), https://doi.org/10.1016/j.ijbiomac.2018.12.273
[45] A. Singh, K. Yadav and A. K. Sen, *Am*. *J*. *Polym*. *Sci*., **2**, 14 (2012)
[46] N. M. Stark, D. J. Yelle and U. P. Agarwal, in "Lignin in Polymer Composites" edited by O. Faruk,

M. Sain, Elsevier, Kidlington, Oxford, 2016, Chapter 4, pp. 49-66
[47] V. Hospodarova, E. Singovszka and N. Stevulova, *Am. J. Anal. Chem.*, **9**, 303 (2018), https://doi.org/10.4236/ajac.2018.96023
[48] B. Abderrahim, E. Abderrahman, A. Mohamed, T. Fatima, T. Abdesselam *et al*., *World J. Environ. Eng.*, **3**, 95 (2015), https://doi.org/10.12691/wjee-3-4-1
[49] W. A. Paixão, L. S. Martins, N. C. Zanini and D. R. Mulinari, *J. Inorg. Organ. Polym. Mater.*, **30**, 2591 (2020)
[50] A. Alakrach, N. Noriman, O. S. Dahham, R. Hamzah, M. A. Alsaadi *et al*., *J. Phys.*, **1019**, 12065 (2018)
[51] A. K. Veeramachineni, T. Sathasivam, S. Muniyandy, P. Janarthanan, S. J. Langford *et al*., *Appl. Sci.*, **6**, 170 (2016), https://doi.org/10.3390/app6060170
[52] R. Nandanwar, A. Haldar, A. Chaudhari and J. Ekhe, *J. Chem. Biol. Phys. Sci.*, **666**, 958 (2016), www.jcbsc.org
[53] T. A. Amit, R. Roy and D. E. Raynie, *Curr. Res. Green Sustain. Chem.*, **4**, 100106 (2021).
[54] B. Shrestha, Y. Le Brech, T. Ghislain, S. B. Leclerc, V. Carré *et al*., *ACS Sustain. Chem. Eng.*, **5**, 6940 (2017), https://doi.org/10.1021/acssuschemeng.7b01130
[55] J. Li, X. Bai, Y. Fang, Y. Chen, X. Wang *et al*., *Combust. Flame*, **215**, 1 (2020), https://doi.org/10.1016/j.combustflame.2020.01.016
[56] L. C. Yeng, M. U. Wahit and N. Othman, *J. Teknol.*, **75**, 11 (2015), https://doi.org/10.11113/jt.v75.5338
[57] A. K. Veeramachineni, T. Sathasivam, S. Muniyandy, P. Janarthanan, S. J. Langford *et al*., *Appl. Sci.*, **6**, 170 (2016), https://doi.org/10.3390/app6060170
[58] H. Li, L. Qi and J. Li, *J. Eng. Fiber. Fabr.*, **12**, 1 (2017), https://doi.org/10.1177/155892501701200201
[59] J. López-Beceiro, A. M. Díaz-Díaz, A. Álvarez-García, J. Tarrío-Saavedra, S. Naya *et al*., *Processes*, **9**, 1154 (2021), https://doi.org/10.3390/pr9071154
[60] J. Domínguez-Robles, T. Tamminen, T. Liitiä, M. S. Peresin, A. Rodríguez *et al*., *Int. J. Biol. Macromol.*, **106**, 979 (2018), https://doi.org/10.1016/j.ijbiomac.2017.08.102
[61] W. Yao, Y. Weng and J. M. Catchmark, *Cellulose*, **27**, 5563 (2020), https://doi.org/10.1007/s10570-020-03177-8
[62] F. Navarro-Pardo, G. Martínez-Barrera, A. L. Martínez-Hernández, V. M. Castaño, J. L. Rivera-Armenta *et al*., *Materials*, **6**, 3494 (2013), https://doi.org/10.3390/ma6083494
[63] A. D. French, *Cellulose*, **27**, 5445 (2020), https://doi.org/10.1007/s10570-020-03172-z
[64] J. He, S. Cui and S. y. Wang, *J. Appl. Polym. Sci.*, **107**, 1029 (2008), https://doi.org/10.1002/app.27061
[65] S. Park, J. O. Baker, M. E. Himmel, P. A. Parilla and D. K. Johnson, *Biotechnol. Biofuels*, **3**, 1 (2010), https://doi.org/10.1186/1754-6834-3-10
[66] A. D. French, *Cellulose*, **21**, 885 (2014), https://doi.org/10.1007/s10570-013-0030-4
[67] O. S. Samuel and A. M. Adefusika, in "Cellulose", edited by A. Rodríguez Pascual and M. E. Eugenio Martín, IntechOpen, 2019, pp. 1-16, https://doi.org/10.5772/intechopen.82849
[68] J. Van Berkum, A. Vermeulen, R. Delhez, T. H. De Keijser and E. Mittemeijer, *J. Appl. Cryst.*, **27**, 345 (1994), https://onlinelibrary.wiley.com/doi/pdf/10.1107/S0021889893010568
[69] M. Wada and T. Okano, *Cellulose*, **8**, 183 (2001), https://doi.org/10.1023/A:1013196220602
[70] A. Goudarzi, L.-T. Lin and F. K. Ko, *J. Nanotech. Eng. Med.*, **5**, 021006 (2014), https://doi.org/10.1115/1.4028300
[71] S. Kubo, Y. Uraki and Y. Sano, *J. Wood Sci.*, **49**, 188 (2003), https://jwoodscience.springeropen.com/counter/pdf/10.1007/s100860300030.pdf
[72] K. B. Ansari and V. G. Gaikar, *Chem. Eng. Sci.*, **115**, 157 (2014)
[73] J.-Y. Kim, H. Hwang, S. Oh, Y.-S. Kim, U.-J. Kim *et al*., *Int. J. Biol. Macromol.*, **66**, 57 (2014), https://doi.org/10.1016/j.ijbiomac.2014.02.013
[74] J. R. Martin, J. F. Johnson and A. R. Cooper, *J. Macromol. Sci.—Rev. Macr. Chem.*, **8**, 57 (1972), https://doi.org/10.1080/15321797208068169
[75] M. Danaei, M. Dehghankhold, S. Ataei, F. Hasanzadeh Davarani, R. Javanmard *et al*., *Pharmaceutics*, **10**, 57 (2018), https://doi.org/10.3390/pharmaceutics10020057
[76] A. K. Gupta, S. Mohanty and S. Nayak, *Materials Focus*, **3**, 444 (2014), https://doi.org/10.1166/mat.2014.1217
[77] A. Jabbarzadeh and B. Halfina, *Nanoscale Adv.*, **1**, 4704 (2019), https://doi.org/10.1039/C9NA00525K
[78] S. Schoenherr, M. Ebrahimi and P. Czermak, in Lignin- Trends and Applications, edited by M. Poletto, IntechOpen, 2018, https://doi.org/10.5772/intechopen.71210